

(SK), who was blinded to the clinical and laboratory findings. Images from all the examinations were stored, and the US scoring reliability was examined in randomly selected patients at the end of the study. This assessment was carried out by JCR-certified rheumatologists (SK, TS, AO, and TO) with consensus. A systematic multiplanar GS and PD examination of 22 joints was performed with the same scanner (TOSHIBA AplioXG) using a multifrequency linear transducer (12 MHz). The US score comprised the following 22 joints: bilateral wrists (intra-carpal, radiocarpal, and ulnocarpal recesses) and finger joints, including the first through fifth metacarpophalangeal (MCP) joints, the first interphalangeal (IP) joint, and the second to fifth proximal interphalangeal (PIP) joints (dorsal recess). Flexor tendons of fingers and six components of extensor tendons of wrists were scanned. All joint regions were sonographically examined in a standardized manner according to the European League Against Rheumatism (EULAR) guidelines [13]. These are the same sites at which MRI has been used to examine patients with early arthritis, as we previously described [9, 15]. US examination of each patient took about 30 min, including documentation.

Each joint was scored for GS and PD on a semiquantitative scale [16] (synovial hypertrophy in GS: grade 0 = absence, no synovial thickening; grade 1 = mild, minimal synovial thickening filling the angle between the periarticular bones without bulging over the line linking the tops of the bones; grade 2 = moderate, synovial thickening bulging over the line linking the tops of the periarticular bones but without extension to at least one bone diaphysis; grade 3 = marked, synovial thickening bulging over the line linking the tops of the periarticular bones and with extension to at least one of the bone diaphyses; PD signals: grade 0 = absence, no synovial flow; grade 1 = mild, single-vessel signals; grade 2 = moderate, confluent signal in less than half of the synovial area; grade 3 = marked, signals in more than half of the synovial area) from 0 to 3, and presence or absence of tenosynovitis was noted. Tenosynovitis is defined by abnormal hypoechoic or anechoic material with or without fluid inside the tendon sheath and with positive PD signals in two perpendicular planes [17]. These scores corresponded to the maximum score for GS and PD obtained from any of the synovial sites evaluated at each joint. The sums of the GS and PD scores obtained from each joint were used as the GS score and PD score (range 0–66), respectively.

MRI examination

Plain MRI of both wrists and finger joints were acquired using a 1.5-T system (Sigma, GE Medical Systems, Milwaukee, WI, USA) with an extremity coil, as we recently

described [9, 15, 18, 19]. Fifty-four patients were examined by MRI within a week of their US evaluation. T1-weighted spin-echo (TR 450, TE 13) images and short-tau inversion recovery (STIR; TR 3000, TE 12, T1 160) images were acquired simultaneously. The images were evaluated for synovitis, bone edema, and bone erosion at 15 sites in each finger and wrist at the distal radioulnar joint, radiocarpal joint, midcarpal joint, first carpometacarpal joint, second through fifth carpometacarpal joints (together), first through fifth metacarpophalangeal joints (separately), and first through fifth proximal interphalangeal joints (PIP joints) separately (for a total of 30 sites in both hands), as we recently reported [9, 15, 18, 19].

Statistical analyses

Within-group comparisons were made using Mann–Whitney's *U* test and the χ^2 test (Fisher's exact probability test when appropriate). The overall significance level for statistical analysis was 5 % (two-sided). *P* values <0.05 were considered statistically significant.

Results

Patient characteristics and diagnoses

The demographic and clinical characteristics of 69 patients are shown in Table 1. Thirty-seven patients (53.6 %) were diagnosed as having RA. Synthetic DMARDs were introduced within the first 3 months to these 37 patients. The initial treatments were methotrexate in 35 patients, sulfasalazine in one, and tacrolimus in one. Thirty-two patients (46.4 %) were diagnosed with other diseases (non-RA) during the follow-up periods, although they could not be classified as non-RA at entry. The diagnoses of these patients were osteoarthritis ($n = 8$), undifferentiated arthritis/arthropathy ($n = 7$), Sjögren syndrome ($n = 4$), polymyalgia rheumatica ($n = 2$), limited-type systemic sclerosis ($n = 2$), tenosynovitis ($n = 2$), reactive arthritis ($n = 1$), polymyositis ($n = 1$), immunoglobulin (Ig)G₄-related disease ($n = 1$), sarcoidosis ($n = 1$), adult T-cell leukemia (ATL), familial Mediterranean fever ($n = 1$), and phalangeal microgeodic syndrome ($n = 1$). The mean disease duration was approximately 4 months in both RA and non-RA patients. The swollen joint counts ($p = 0.0104$) and CRP ($p = 0.0003$) and ESR ($p = 0.0009$) values were higher in RA patients than in non-RA patients, but the tender joint counts were not different. The seropositive rates of RF (70.3 %, $p = 0.0002$) and ACPA (62.2 %, $p < 0.0001$) were significantly higher in RA than in non-RA patients. Patients with high MMP-3 were also predominantly distributed in the RA group (48.6 %, $p = 0.0432$).

Comparison of MSKUS findings between RA and non-RA patients

The MSKUS findings in RA and non-RA patients are shown in Table 2. The rates at which GS grade ≥ 1 ($p = 0.0005$), GS grade ≥ 2 ($p < 0.0001$), GS grade = 3 ($p < 0.0001$), PD grade ≥ 1 ($p < 0.0001$), and PD grade ≥ 2 ($p < 0.0001$) were present at any joint were significantly higher in RA than in non-RA patients. However, GS grade ≥ 1 , GS grade ≥ 2 , and PD grade ≥ 1 also occurred in non-RA patients, as 23 (71.9 %), 12 (37.5 %), and ten (31.3 %) patients were positive for the above grades, respectively, out of 32 non-RA patients. The occurrence of PD grade = 3 was specific to RA patients; however, it was only found in four of 37 RA patients (10.8 %). Both GS and PD scores were significantly higher in RA than in non-RA patients. The frequency of findings of tenosynovitis was prominent in the RA group, but the difference from the frequency in the non-RA group was not significant. Bone erosions were specifically detected in RA patients; however, the rate was not high (18.9 %, $p = 0.0094$). Accordingly, PD grade ≥ 2 at any joint is considered to be most important MSKUS findings in RA patients.

Comparison of plain MRI findings between RA and non-RA patients

The plain MRI findings in RA and non-RA patients are also shown in Table 2. As most patients with RA expressed symmetrical synovitis that was also found in non-RA patients, we could not find statistical significance in this result. As suspected, bone edema was significantly distributed in the RA group compared with the non-RA group; however, that was not so remarkable compared with MSKUS findings. Patients with MRI-proven bone erosion tended to be distributed in the RA group, but the difference did not reach statistical significance ($p = 0.0838$).

Laboratory data, MSKUS findings, MRI findings, and 2010 RA classification criteria for the diagnosis of RA

Sensitivity, specificity, and accuracy of laboratory data, MSKUS findings, MRI findings, and 2010 RA classification criteria are shown in Table 3. The presence of ACPA was the most specific laboratory data distributed in patients with RA. Surprisingly, the presence of MSKUS findings, especially the presence of PD grade 2 or 3 at any joint, was very specific in

Table 1 Demographic, clinical, and laboratory characteristics at baseline

	RA (N = 37)	Non-RA (N = 32)	P value
Age (years ^a)	53.6 ± 17.2	54.5 ± 12.5	NS
Female/male (n)	28/9	26/6	NS
Durations of symptom (months ^a)	4.0 ± 3.0	3.7 ± 2.9	NS
≥ 1.5 months/ < 1.5 months	31/6	24/8	NS
Tender joint counts (n ^a)	7.9 ± 7.6	5.6 ± 6.9	NS
Swollen joint counts (n ^a)	5.6 ± 6.9	3.4 ± 6.3	0.0104
CRP			
Positive/negative	24/13	8/24	0.0009
Value (mg/dl ^a)	1.29 ± 2.94	0.40 ± 1.09	0.0003
ESR			
Positive/negative	27/10	11/21	0.0013
Value (mm/h ^a)	32.2 ± 24.5	18.0 ± 20.6	0.0009
CRP and/or ESR			
Positive/negative	31/6	13/19	0.0002
RF			
Positive/negative	26/11	8/24	0.0002
Titers: $> \times 3 / \leq \times 3$	17/20	3/29	0.0083
ACPA			
Positive/negative	23/14	2/30	1.4×10^{-6}
Titers: $> \times 3 / \leq \times 3$	23/14	1/31	2.8×10^{-7}
IgM-RF and/or ACPA			
Positive/negative	27/10	9/23	0.0002
Titers: $> \times 3 / \leq \times 3$	23/14	4/28	2.5×10^{-5}
MMP-3			
Positive/negative	18/19	8/24	0.0432

Within-group comparisons were assessed with Mann–Whitney’s U test and the χ^2 test (Fisher’s exact probability test when appropriate)

NS not significant, RF rheumatoid factor, ACPA anti-CCP antibody, MMP-3 matrix metalloproteinase-3

^a Mean ± standard deviation

Table 2 Ultrasonography and MRI findings at baseline

	RA (N = 37)	Non-RA (N = 32)	P value
MSKUS			
Gray-scale			
Grade ≥ 1 presence/absence	37/0	23/9	0.0005
Grade 2 or 3 presence/absence	33/4	12/20	6.9×10^{-6}
Grade 3 presence/absence	21/16	1/31	1.9×10^{-6}
Total GS score (0–66) ^a	9.4 ± 7.6	3.7 ± 4.0	0.0001
Power Doppler			
Grade ≥ 1 presence/absence	34/3	10/22	1.7×10^{-7}
Grade 2 or 3 presence/absence	30/7	2/30	5.1×10^{-10}
Grade 3 presence/absence	4/33	0/32	0.0764
Total PD score (0–66) ^a	4.2 ± 3.7	0.6 ± 1.1	9.7×10^{-9}
Tenosynovitis			
Presence/absence	21/16	6/26	0.0013
Bone erosion			
Presence/absence	7/30	0/32	0.0094
	RA (N = 32)	Non-RA (N = 22)	P value
MRI			
Symmetrical synovitis			
Presence/absence	28/4	16/6	NS
Bone edema			
Presence/absence	15/17	4/18	0.0300
Bone erosion			
Presence/absence	9/23	2/20	0.0838

Within-group comparisons were assessed with Mann–Whitney's *U* test and the χ^2 test (Fisher's exact probability test when appropriate)

RA rheumatoid arthritis, MSKUS musculoskeletal ultrasonography, GS gray-scale, PD power Doppler, MRI magnetic resonance imaging, NS not significant

^a Mean \pm standard deviation

RA. If we considered patients to have RA in cases in which MSKUS findings showed PD grade 2 or 3, the diagnostic performance of MSKUS for RA had sensitivity 81.1 %, specificity 93.8 %, positive predictive value (PPV) 93.8 %, negative predictive value (NPV) 81.1 %, and accuracy 87.0 %. The 2010 RA classification criteria classified RA with sensitivity 59.5 %, specificity 87.5 %, PPV 84.6 %, NPV 65.1 %, and accuracy 72.5 %, suggesting that the presence of PD grade 2 or 3 may have been more specific than the 2010 RA classification criteria. In accordance with data shown in Table 2, MRI-proven bone edema could not differentiate RA from non-RA compared with PD grading.

We tried to combine 2010 RA classification criteria with the PD grade 2 or 3 rule for the clinical diagnosis of RA, and the results are shown in Fig. 1. We initially applied 2010 RA classification criteria, and if the patients did not fulfill those criteria, the PD grade 2 or 3 rule was introduced. We found that this decision tree can differentiate patients more efficiently than can the PD grade 2 or 3 rule alone.

Discussion

The authors of previous assessments of the performance of the 2010 RA classification criteria have usually tried to

identify patients with RA as those who were treated with DMARDs within the first year of the follow-up period [20–23]. As of this writing, the 2010 RA classification criteria were published last year and are going to be applied in the clinical field of rheumatology. Rheumatologists tend to start DMARDs earlier in patients who are expected to develop erosive arthritis. Therefore, in this study, we considered patients to have RA if their physicians had started DMARDs within the first 3 months. This clinical setting may clarify more definitely which patients should be considered to have RA for the purpose of applying the T2T strategy that has come to be widely recommended.

Diagnostic performance of the 2010 RA classification criteria in this study was fairly good, with both the specificity and PPV around 85 %. As this was a prospective investigator-initiated clinical study, physicians were able to choose the treatment at every visit according to the clinical status of patients fulfilling the 2010 RA classification criteria. Thus, the score according to the 2010 RA classification criteria at each visit may be directly involved in the physician's decision, which associated with the increment of specificity and PPV of the 2010 RA classification criteria. However, the levels of other components, such as sensitivity, NPV, and accuracy, were not high, indicating that additional procedures may be necessary to assist the

Table 3 Performance of laboratory data, ultrasonography findings, and 2010 rheumatoid arthritis (RA) classification criteria

	Sensitivity (%)	Specificity (%)	PPV (%)	NPV (%)	Accuracy (%)
Laboratory data					
CRP (positive)	64.9	75.0	75.0	64.9	69.6
ESR (positive)	73.0	65.6	71.1	67.7	69.6
RF (positive)	70.3	75.0	76.5	68.6	72.5
ACPA (positive)	62.2	93.8	92.0	68.2	76.8
MMP-3 (positive)	48.6	75.0	69.2	55.8	60.9
MSKUS					
Gray-scale; grade ≥ 1	100	28.1	61.7	100	66.7
Gray-scale; grade 2 or 3	89.2	62.5	73.3	83.3	76.8
Gray-scale; grade 3	56.8	96.9	95.5	66.0	75.4
Power Doppler; grade ≥ 1	91.9	68.8	77.3	88.0	81.2
Power Doppler; grade 2 or 3	81.1	93.8	93.8	81.1	87.0
Power Doppler; grade 3	10.8	100	100	49.2	52.2
Tenosynovitis (positive)	56.8	81.3	77.8	61.9	68.1
Bone erosion (positive)	18.9	100	100	51.6	56.5
MRI					
Symmetrical synovitis (positive)	87.5	27.3	63.6	60.0	63.0
Bone edema (positive)	46.9	81.8	78.9	51.4	61.1
Bone erosion (positive)	28.1	90.9	81.8	46.5	53.7
2010 RA classification criteria	59.5	87.5	84.6	65.1	72.5

RF rheumatoid factor, ACPA anti-CCP antibody, MMP-3 matrix metalloproteinase-3, MSKUS musculoskeletal ultrasound, PPV positive predictive value, NPV negative predictive value, MRI magnetic resonance imaging

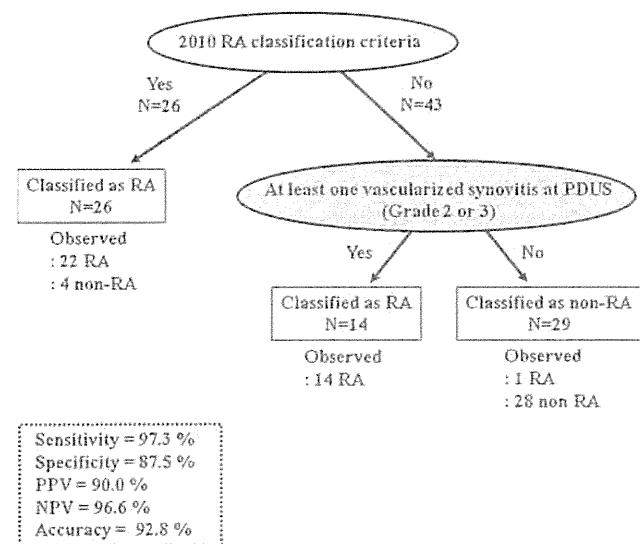


Fig. 1 Decision tree algorithm for diagnosis of early arthritis patients by 2010 rheumatoid arthritis (RA) classification criteria in conjunction with power Doppler PD grade 2 or 3; 2010 RA criteria were initially applied to 69 patients. If the patients fulfilled the criteria, they were classified as having RA (26 patients). PD grade 2 or 3 rule was applied for the remaining 43 patients. This tree algorithm classified patients as having RA at sensitivity 97.3 %, specificity 7.5 %, positive predictive value (PPV) 90.0 %, negative predictive value (NPV) 96.6 %, and accuracy 92.8 %

diagnostic performance of the 2010 RA classification criteria.

In this regard, we focused on MSKUS, as it is more sensitive and reliable than clinical examination for detecting joint injury in patients with RA [5–8]. Synovitis, tenosynovitis, and bone erosion are the major joint injuries that are frequently found in patients with RA examined by MSKUS [5–8, 10–13]. GS determines the hypertrophy of synovial tissues, whereas PD identifies vascularity [5–8, 10–13]. In our study, PD grade, especially grade 2 or 3, was highly specific in patients with RA. These data are consistent with the previous findings that the synovial vascularity determined by PD reflects RA disease activity more efficiently than do GS findings [24, 25]. The levels of statistical components were even better than those of the 2010 RA classification criteria, indicating that the presence of severe and active synovial inflammation detected by PD may deeply affect physicians’ decisions to start DMARDs.

Although the US examiner was always blinded to the clinical and laboratory findings of patients in this study, physicians could take into consideration the results of US for the choice of DMARDs at each point. Therefore, it could also be said that PD overestimates the presence of RA and thus influences the initiation of or choice of DMARDs that was directly associated with our data. As for

MRI, the presence of bone edema is thought to be the most suitable indicator for a clinical diagnosis of RA. These results are consistent with our previous report that bone edema is able to predict the development of RA that fulfills the 1987 classification criteria from patients with early arthritis more efficiently than symmetrical synovitis and bone erosion [15]. As physicians judge patients as having RA based on findings of not only MSKUS but also MRI, we could state that PD grade 2 or 3 is superior to bone edema on plain MRI for making a clinical diagnosis of RA. If we obtain gadolinium-diethylenetriamine pentaacetic acid (Gd-DTPA)-enhanced MRI instead of plain MRI, bone edema may be more significantly involved in RA diagnosis. In our previous study, we found that the detection sensitivity of bone edema on plain MRI is 30 % less than that with Gd-DTPA-enhanced MRI [15]. We therefore propose a tree algorithm for clinical RA diagnosis that combines the 2010 RA classification criteria and PD, as shown in Fig. 1. This kind of approach can also be applied in patients with spondyloarthropathy, indicating that Amor's criteria in conjunction with vascularized entheses bring good results [26]. Accordingly, our data identify that the tree algorithm shown in Fig. 1 can classify more patients as having RA at a high discriminative value compared with the 2010 RA classification criteria or PD alone, supposing more patients received the chance of early introduction of DMARDs. Our data may also indicate that the combination of physical examination and serology with a sensitive imaging technique, such as MSKUS, is the best way to identify erosive disease early. Filer et al. [7] reported that a combination of Leiden score, but not the 2010 RA classification criteria, with MSKUS-proven synovitis improved in clinical RA diagnosis. Our data may follow that result. Long-term follow-up and larger studies are warranted to confirm that MSKUS, especially PD, in combination with the 2010 RA classification criteria, is valuable for early identification of patients with erosive RA

Conflict of interest None.

References

- Smolen JS, Aletaha D, Bijlsma JW, Breedveld FC, Boumpas D, Burmester G, et al. Treating rheumatoid arthritis to target: recommendations of an international task force. *Ann Rheum Dis*. 2010;69:631–7.
- Smolen JS, Landewé R, Breedveld FC, Dougados M, Emery P, Gaujoux-Viala C, et al. EULAR recommendations for the management of rheumatoid arthritis with synthetic and biological disease-modifying antirheumatic drugs. *Ann Rheum Dis*. 2010;69:964–75.
- Arnett FC, Edworthy SM, Bloch DA, McShane DJ, Fries JF, Cooper NS, et al. The American Rheumatism Association 1987 revised criteria for the classification of rheumatoid arthritis. *Arthritis Rheum*. 1988;31:315–24.
- Aletaha D, Neogi T, Silman AJ, Funovits J, Felson DT, Bingham CO 3rd, et al. 2010 rheumatoid arthritis classification criteria: an American College of Rheumatology/European League Against Rheumatism collaborative initiative. *Arthritis Rheum*. 2010;62:2569–81.
- Naredo E, Bonilla G, Gamero F, Uson J, Carmona L, Laffon A. Assessment of inflammatory activity in rheumatoid arthritis: a comparative study of clinical evaluation with grey scale and power Doppler ultrasonography. *Ann Rheum Dis*. 2005;64:375–81.
- Salaffi F, Filippucci E, Carotti M, Naredo E, Meenagh G, Ciapetti A, et al. Inter-observer agreement of standard joint counts in early rheumatoid arthritis: a comparison with grey scale ultrasonography—a preliminary study. *Rheumatology (Oxford)*. 2008;47:54–8.
- Filer A, de Pablo P, Allen G, Nightingale P, Jordan A, Jobanputra P, et al. Utility of ultrasound joint counts in the prediction of rheumatoid arthritis in patients with very early synovitis. *Ann Rheum Dis*. 2011;70:500–7.
- Saleem B, Brown AK, Keen H, Nizam S, Freeston J, Karim Z, et al. Disease remission state in patients treated with the combination of tumor necrosis factor blockade and methotrexate or with disease-modifying antirheumatic drugs: a clinical and imaging comparative study. *Arthritis Rheum*. 2009;60:1915–22.
- Tamai M, Kawakami A, Iwamoto N, Kawashiri SY, Fujikawa K, Aramaki T, et al. Comparative study of the detection of joint injury in early-stage rheumatoid arthritis by MRI of wrist and finger joints and physical examination. *Arthritis Care Res (Hoboken)*. 2011;63:436–9.
- Østergaard M, Pedersen SJ, Døhn UM. Imaging in rheumatoid arthritis—status and recent advances for magnetic resonance imaging, ultrasonography, computed tomography and conventional radiography. *Best Pract Res Clin Rheumatol*. 2008;22:1019–44.
- Naredo E, Collado P, Cruz A, Palop MJ, Cabero F, Richi P, et al. Longitudinal power Doppler ultrasonographic assessment of joint inflammatory activity in early rheumatoid arthritis: predictive value in disease activity and radiologic progression. *Arthritis Rheum*. 2007;57:116–24.
- Wakefield RJ, Gibbon WW, Conaghan PG, O'Connor P, McGonagle D, Pease C, et al. The value of sonography in the detection of bone erosions in patients with rheumatoid arthritis: a comparison with conventional radiography. *Arthritis Rheum*. 2000;43:2762–70.
- Backhaus M, Burmester GR, Gerber T, Grassi W, Machold KP, Swen WA, Working Group for Musculoskeletal Ultrasound in the EULAR Standing Committee on International Clinical Studies including Therapeutic Trials, et al. Guidelines for musculoskeletal ultrasound in rheumatology. *Ann Rheum Dis*. 2001;60:641–9.
- Kawashiri SY, Kawakami A, Iwamoto N, Fujikawa K, Satoh K, Tamai M, et al. The power Doppler ultrasonography score from 24 synovial sites or 6 simplified synovial sites, including the metacarpophalangeal joints, reflects the clinical disease activity and level of serum biomarkers in patients with rheumatoid arthritis. *Rheumatology (Oxford)*. 2011;50:962–5.
- Tamai M, Kawakami A, Uetani M, Takao S, Arima K, Iwamoto N, et al. A prediction rule for disease outcome in patients with undifferentiated arthritis using magnetic resonance imaging of the wrists and finger joints and serologic autoantibodies. *Arthritis Rheum*. 2009;61:772–8.
- Szkudlarek M, Court-Payen M, Jacobsen S, Klarlund M, Thomsen HS, Østergaard M. Interobserver agreement in ultrasonography of the finger and toe joints in rheumatoid arthritis. *Arthritis Rheum*. 2003;48:955–62.
- Backhaus M. Ultrasound and structural changes in inflammatory arthritis: synovitis and tenosynovitis. *Ann N Y Acad Sci*. 2009;1154:139–51.

18. Kita J, Tamai M, Arima K, et al. Delayed treatment with tumor necrosis factor inhibitors in incomplete responders to synthetic disease-modifying anti-rheumatic drugs shows an excellent effect in patients with very early rheumatoid arthritis with poor prognosis factors. *Mod Rheumatol*. 2011 (Epub ahead of print).
19. Kita J, Tamai M, Arima K, et al. Treatment discontinuation in patients with very early rheumatoid arthritis in sustained simplified disease activity index remission after synthetic disease-modifying anti-rheumatic drug administration. *Mod Rheumatol*. 2011 (Epub ahead of print).
20. van der Linden MP, Knevel R, Huizinga TW, van der Helm-van Mil AH. Classification of rheumatoid arthritis: comparison of the 1987 American College of Rheumatology criteria and the 2010 American College of Rheumatology/European League Against Rheumatism criteria. *Arthritis Rheum*. 2011;63:37–42.
21. Kaneko Y, Kuwana M, Kameda H, Takeuchi T. Sensitivity and specificity of 2010 rheumatoid arthritis classification criteria. *Rheumatology (Oxford)*. 2011;50:1268–74.
22. Britsemmer K, Ursum J, Gerritsen M, van Tuyl L, van Schaardenburg D. Validation of the 2010 ACR/EULAR classification criteria for rheumatoid arthritis: slight improvement over the 1987 ACR criteria. *Ann Rheum Dis*. 2011;70:1468–70.
23. Cader MZ, Filer A, Hazlehurst J, de Pablo P, Buckley CD, Raza K. Performance of the 2010 ACR/EULAR criteria for rheumatoid arthritis: comparison with 1987 ACR criteria in a very early synovitis cohort. *Ann Rheum Dis*. 2011;70:949–55.
24. Joshua F, Edmonds J, Lassere M. Power Doppler ultrasound in musculoskeletal disease: a systematic review. *Semin Arthritis Rheum*. 2006;36:99–108.
25. Freeston JE, Wakefield RJ, Conaghan PG, Hensor EM, Stewart SP, Emery P. A diagnostic algorithm for persistence of very early inflammatory arthritis: the utility of power Doppler ultrasound when added to conventional assessment tools. *Ann Rheum Dis*. 2010;69:417–9.
26. D'Agostino MA, Aegerter P, Bechara K, Salliot C, Judet O, Chimenti MS, et al. How to diagnose spondyloarthritis early? Accuracy of peripheral enthesitis detection by power Doppler ultrasonography. *Ann Rheum Dis*. 2011;70:1433–40.

TLR3-mediated apoptosis and activation of phosphorylated Akt in the salivary gland epithelial cells of primary Sjögren's syndrome patients

Hideki Nakamura · Yoshiro Horai · Takahisa Suzuki · Akitomo Okada · Kunihiro Ichinose · Satoshi Yamasaki · Takehiko Koji · Atsushi Kawakami

Received: 4 October 2011 / Accepted: 11 March 2012 / Published online: 29 March 2012
© Springer-Verlag 2012

Abstract This study aimed to ascertain whether innate immunity is involved in the apoptosis of primary cultured salivary gland epithelial cells (SGECs) in primary Sjögren's syndrome (pSS). Induction of apoptosis of SGECs was performed using a TLR3 ligand, poly (I:C). Activation of phosphorylated-Akt (pAkt) and cleaved-caspase 3 was determined by Western blotting or immunofluorescence. Expression of TLR2 and TLR3 with pAkt was observed in cultured SGECs after 24-h stimulation with each ligand. Compared with stimulation with the peptidoglycan or lipopolysaccharide, that with poly (I:C) induced significant nuclear fragmentation, as determined by Hoechst staining ($p = 0.0098$). Apoptosis was confirmed by terminal deoxynucleotidyltransferase-mediated dUTP nick end-labeling (TUNEL) staining of SGECs from pSS patients and a normal subject. A significant increase in TUNEL-positive cells was observed by the addition of a PI3K inhibitor, LY294002. Poly (I:C) phosphorylated stress-activated protein kinase/Jun-terminal kinase and p44/42 MAP kinase as well as Akt. Furthermore, poly (I:C)-induced caspase 3 cleavage in SGECs was also inhibited by LY294002. Similar results were obtained using SGECs obtained from a normal subject. The results demonstrated for the first time that TLR3 induces

the apoptotic cell death of SGECs via the PI3K-Akt signaling pathway.

Keywords Sjögren's syndrome · TLR3 · Akt · MAP kinase · Caspase3

Abbreviations

IFN	Interferon
IRF3	Interferon (IFN) regulatory factor 3
FITC	Fluorescein isothiocyanate
LPS	Lipopolysaccharide
LSG	Labial salivary gland
MAP	Mitogen-activated protein
PBS	Phosphate-buffered saline
PGN	Peptidoglycan
PI3K	Phosphatidylinositol 3-kinase
pSS	Primary Sjögren's syndrome
SGECs	Salivary gland epithelial cells
TRIF	TIR domain-containing adaptor-inducing IFN β
TRITC	Tetramethyl rhodamine isothiocyanate
TUNEL	Terminal deoxynucleotidyltransferase-mediated dUTP nick end-labeling

H. Nakamura (✉) · Y. Horai · T. Suzuki · A. Okada · K. Ichinose · S. Yamasaki · A. Kawakami
Unit of Translational Medicine, Department of Immunology and Rheumatology, Nagasaki University Graduate School of Biomedical Sciences, 1-7-1 Sakamoto, Nagasaki City, Nagasaki 852-8501, Japan
e-mail: nhideki@nagasaki-u.ac.jp

T. Koji
Department of Histology and Cell Biology,
Nagasaki University Graduate School of Biomedical Sciences,
Nagasaki City, Nagasaki 852-8501, Japan

Introduction

Toll-like receptors (TLRs) are known as intermediation receptors involved in innate immunity [1]. Some TLRs are signaling adaptor molecules that are stimulated by bacterial or viral nucleic acid sequences [2, 3]. We previously reported the expression of TLR2, 3, and 4 in labial salivary glands (LSGs) obtained from patients with primary Sjögren's syndrome (pSS) [4] showing sicca symptoms due to salivary gland destruction [5, 6]. These three types of TLRs

have been shown to be expressed in a human salivary gland (HSG) cell line, as well as in LSGs from pSS patients in vitro [4]. Additionally, in vitro stimulation of an immortalized human salivary gland cell line, HSG cells, with TLR ligands did not induce Akt phosphorylation but rather the phosphorylation of mitogen-activated protein kinases (MAPKs) [4]. However, no detailed kinetic analyses of apoptotic signals and Akt activation in cultured primary salivary gland epithelial cells (SGECs) of pSS patients have been conducted to date. In our series of studies, apoptotic sensitivity to pro-apoptotic signaling in SGECs differed from that in HSGs [7, 8]. For instance, a significant difference in sensitivity to anti-Fas antibody was observed between these cell types. Although HSGs showed sensitivity to a single stimulation with anti-Fas antibody, cultured SGECs required stimulation with both anti-Fas antibody and phosphoinositide-3-kinase (PI3K) inhibitor to induce apoptosis [7]. Since recent studies have shown that TLRs can induce apoptosis in certain types of cells such as human breast tumor cells [9, 10], it is reasonable to speculate that SGECs and HSGs may respond differently to TLR ligands. Thus, findings obtained thus far with SGECs appear to be more relevant to the clinical setting than those of series using HSGs. In the present study, we investigated TLR-mediated cell death and the expression of relevant anti-apoptotic molecules in the SGECs of pSS patients.

Materials and methods

Patients

This study contained three female patients with pSS (age: 62.7 ± 4.7). Diagnosis of pSS was determined by the revised criteria proposed by the American-European Consensus Group [11, 12]. SGECs obtained from a 59-year-old female who showed sicca symptoms without a diagnosis of pSS were used as the normal control. Labial salivary gland (LSG) biopsies were performed after informed consent was obtained from all participants. The study was conducted in accordance with the human experimental guidelines of our institution.

Antibodies and reagents

Anti-cleaved caspase 3 rabbit monoclonal antibody, phosphorylated-Akt S⁴⁷³, phosphorylated stress-activated protein kinase/Jun-terminal kinase (SAPK/JNK), phosphorylated p38 MAP kinase, and phosphorylated p44/42 MAP kinase rabbit polyclonal antibodies were purchased from Cell Signaling Technology, Inc. (Danvers, MA, USA). Polyclonal goat anti-TLR2, 3, and 4 antibodies

were purchased from Santa Cruz Biotechnology (Santa Cruz, CA, USA). Secondary antibodies including donkey anti-mouse IgG conjugated with fluorescein isothiocyanate (FITC) and donkey anti-rabbit IgG conjugated with tetramethyl rhodamine isothiocyanate (TRITC) were purchased from Jackson ImmunoResearch Laboratories, Inc. (West Grove, PA, USA). Hoechst dye 33258 was purchased from Sigma (St. Louis, MO, USA). The selective PI3K inhibitor LY294002 was purchased from Calbiochem (La Jolla, CA, USA). Peptidoglycan (PGN) from *Staphylococcus aureus* and poly (I:C) were purchased from InvivoGen (San Diego, CA, USA) and lipopolysaccharide (LPS) from *Escherichia coli* was purchased from Sigma (St. Louis, MO, USA).

Culture of primary salivary epithelial cells

The method used for culturing SGECs from pSS patients has been described in our previous reports [7, 8]. Briefly, minor salivary gland tissue was excised and cultured in a defined keratinocyte-SFM culture medium (Invitrogen Life Technologies, Carlsbad, CA, USA) supplemented with hydrocortisone (Sigma) and bovine pituitary extract (Kurobo, Osaka, Japan). For immunofluorescence studies, the SGECs were cultured on 12-mm² cover slips that were prospectively coated with a Type I collagen, Cellmatrix (Nitta Gelatin, Inc., Osaka, Japan).

Immunofluorescence

The SGECs on 12-mm² cover slips were incubated for 10 min in PBS containing 4 % paraformaldehyde at 4 °C, and the cells were subsequently immersed in methanol at −20 °C for 10 min. After the reaction was blocked in 5 % normal horse serum in PBS, the SGECs were incubated in the primary antibodies for 1 h at room temperature. After the cells were washed three times in PBS, the SGECs were incubated with FITC-labeled and TRITC-labeled secondary antibodies in medium supplemented with Hoechst dye 33258 under dark conditions. After incubation with the secondary antibodies, the SGECs were mounted in Vectashield mounting medium (Vector Laboratories, Inc., Burlingame, CA, USA), and were scanned by confocal microscopy (LSM5, PASCAL; Carl Zeiss, Jena, Germany). Control experiments were performed to confirm the isotype specificity of the secondary antibodies.

Induction of apoptosis

After 12 h of growth-supplement starvation, the primary cultured SGECs were treated with poly (I:C) (final concentration: 25 µg/ml) for 24 h.

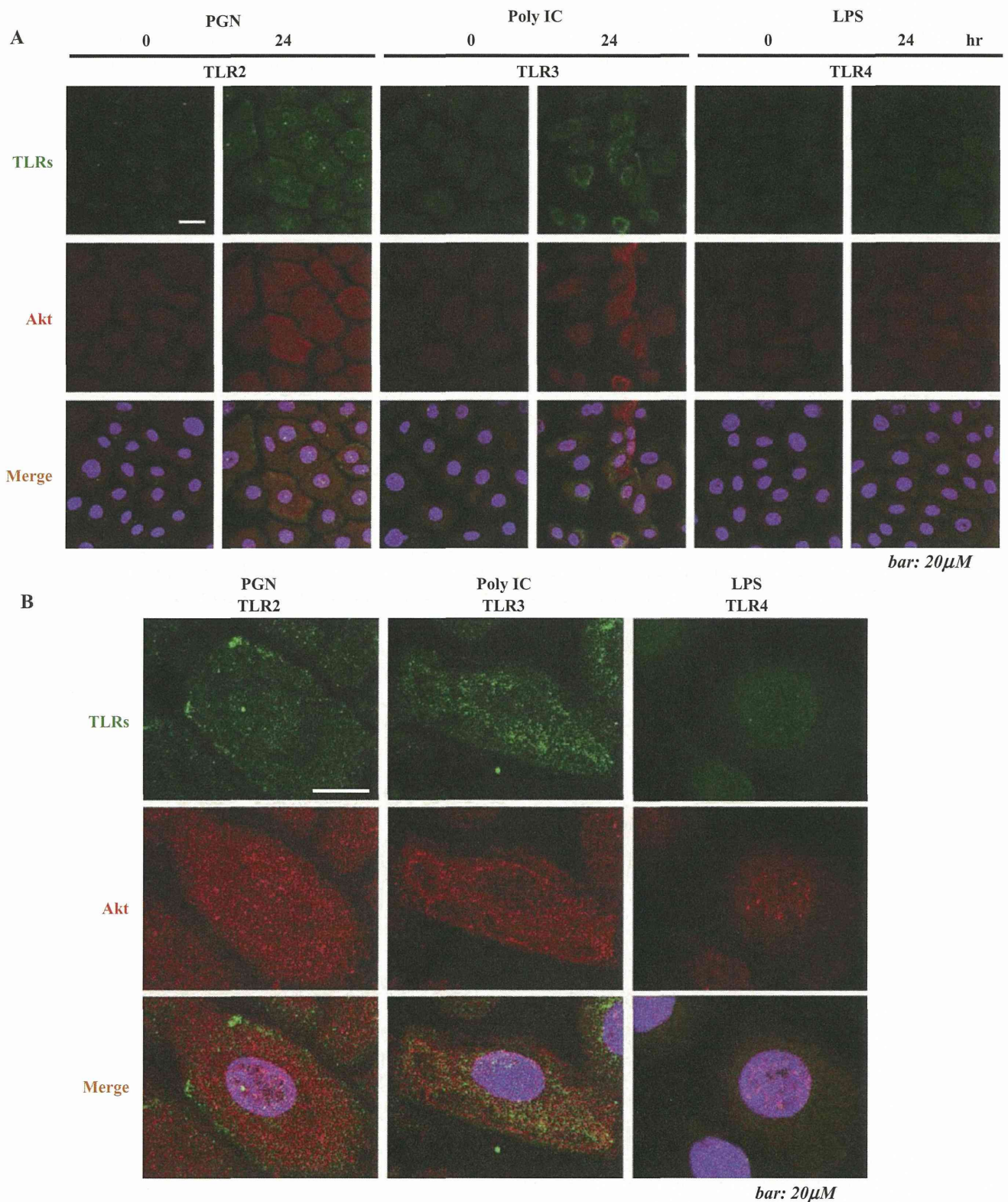


Fig. 1 Expression of TLRs in the presence of their ligands in primary cultured salivary gland epithelial cells (SGECs). After 12 h of starvation of growth supplement, primary cultured SGECs were treated with 10 μg/ml of PGN, 25 μg/ml of poly (I:C), or 1 μg/ml of LPS for 24 h (low magnification; **a**). The SGECs were double-labeled using goat anti-TLR2, 3, or 4 antibody with FITC-conjugated

secondary antibody (*green*) and rabbit anti-phosphorylated Akt antibody with tetramethyl rhodamine isothiocyanate (TRITC)-conjugated secondary antibody (*red*). The status of the nucleus was observed by Hoechst staining (*blue*). **b** A higher-magnification view after 24-h stimulation with each ligand. Shown are the representative results of three independent experiments (*bar*, 20 μM)

Terminal deoxynucleotidyltransferase-mediated dUTP nick end-labeling (TUNEL) staining

For the detection of apoptosis, TUNEL staining was employed to demonstrate double-stranded DNA breaks, as shown in our previous study [13]. Later, the SGECs were fixed in 4 % PFA 4 °C for 15 min followed by immersion in PBS with 0.5 % Tween 20 and 0.2 % bovine serum albumin using the MEBSTAIN Apoptosis kit Direct (MBL, Nagoya, Japan). The SGECs were incubated with a 50 μ l terminal deoxynucleotidyl transferase (TdT) solution at 37 °C for 1 h. The stained SGECs were captured by confocal microscopy and analyzed by WinROOF software (Mitani Corporation, Fukui, Japan) [14].

Western blot analysis

The method used for Western blot analysis has also been described in our previous reports [8]. Briefly, the SGECs were lysed and the protein concentrations were determined, and identical amounts of protein were subjected to 12.5 % sodium dodecyl sulfate–polyacrylamide gel electrophoresis (SDS-PAGE). After the proteins were transferred to a polyvinylidene fluoride filter, blocking for 1 h using 5 % nonfat dried milk in Tris-buffered saline containing 0.1 % Tween 20 was performed, after which the cells were incubated at 4 °C overnight with anti-cleaved caspase 3 rabbit monoclonal antibody, phosphorylated-Akt S⁴⁷³, phosphorylated stress-activated protein kinase/Jun-terminal

kinase (SAPK/JNK), phosphorylated p38 MAP kinase, and phosphorylated p44/42 MAP kinase rabbit polyclonal antibodies. After incubation with a 1:1,000 dilution of donkey anti-rabbit IgG, coupled with horseradish peroxidase, detection with an enhanced chemiluminescence (ECL) system (Amersham, Arlington Heights, IL, USA) was performed. For statistical analysis, the Student's *t* test was used ($p < 0.05$; considered as statistically significant).

Results

Expression of TLRs and phosphorylated Akt in primary SGECs with TLR ligand stimulation

We initially examined the expression of three types of TLR in primary cultured SGECs stimulated by TLR ligands (Fig. 1a). Although TLR2 and TLR3 were detected in the cell membrane or cytoplasm in the presence of PGN and poly (I:C), no TLR4 signal was detected (Fig. 1b). Phosphorylated Akt was also detected in the presence of PGN and poly (I:C).

Frequency of nuclear fragmentation under the presence of TLR ligands in primary SGEC from pSS patients and a normal subject

Nuclear fragmentation was detected using Hoechst staining in pSS patients. When 100 cells in three different fields

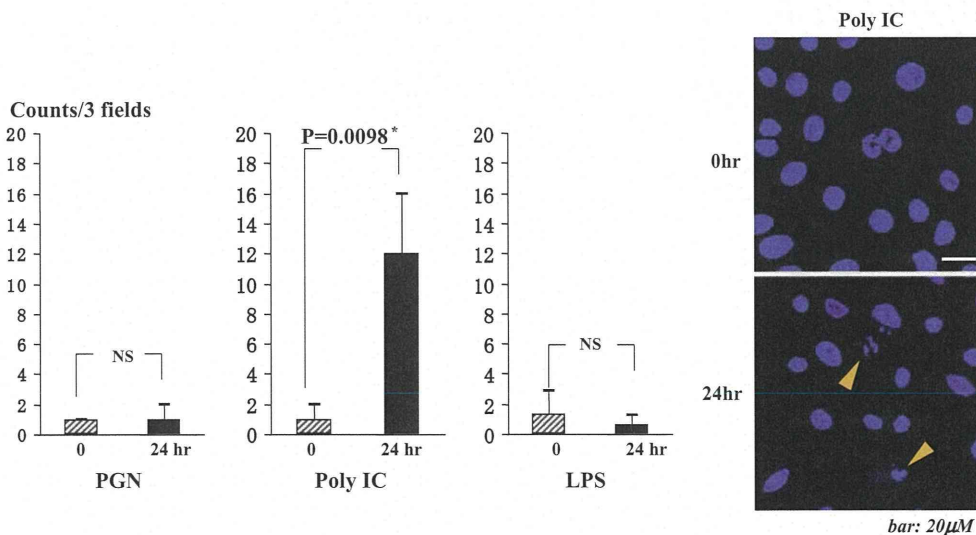


Fig. 2 Nuclear fragmentation induced by poly (I:C) in primary cultured salivary gland epithelial cells (SGECs). After 12 h of starvation of growth supplement, primary cultured SGECs were treated with 10 μ g/ml of PGN, 25 μ g/ml of poly (I:C), or 1 μ g/ml of LPS for 24 h. Then, to quantify nuclear fragmentation identified by Hoechst staining, 100 cells of interest were counted in three different fields. In the *left panel*, the average number of cell deaths observed

among poly (I:C)-stimulated cells was statistically compared with that of PGN or LPS-stimulated cells, as evaluated by unpaired Student's *t* test ($p < 0.05$; statistically significant). *NS* not significant. Shown are the representative results of two independent experiments. The *right panel* shows representative nuclear fragmentation (*arrowheads*) induced by poly (I:C)

were counted to quantify the fragmented cells, poly (I:C) stimulation induced a statistically significant amount of fragmentation (p value = 0.0098, determined by Student’s t test, $p < 0.05$; statistically significant) compared with that induced by PGN or LPS (Fig. 2, left panel). For the normal subject, poly (I:C) stimulation also induced significant nuclear fragmentation (p value = 0.0023). A representative fragmentation in a pSS patient was observed (Fig. 2, right panel).

Detection of poly (I:C)-induced apoptosis by TUNEL assay

TUNEL staining was employed to determine whether the fragmentation determined by Hoechst staining was due to cell death. Twenty-four hours after stimulation with poly (I:C) in SGECs from pSS patients, nuclear fragmentation was detected by bright-field and Hoechst staining. The Hoechst-positive cells were merged, as shown by TUNEL

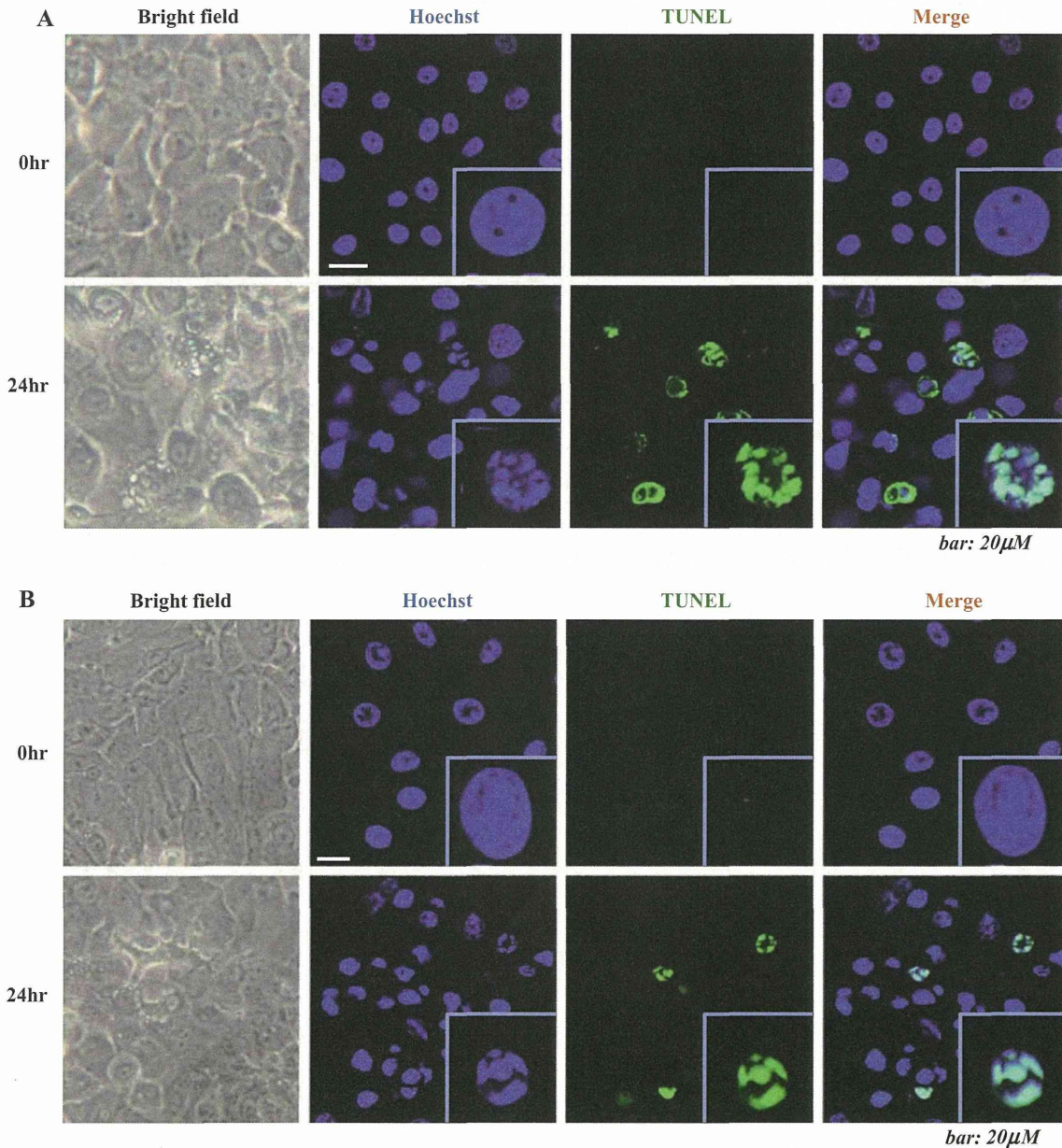


Fig. 3 Detection of double-stranded DNA breakage by terminal deoxynucleotidyltransferase-mediated dUTP nick end-labeling (TUNEL) staining in primary cultured salivary gland epithelial cells (SGECs). After 12 h of starvation of growth supplement, primary cultured SGECs were treated with 25 μg/ml of poly (I:C) for 24 h. To confirm apoptosis as a double-stranded DNA break at the site of

nuclear fragmentation, we employed TUNEL-staining coupled with bright-field view. **a, b** The results from a pSS patient and a normal subject, respectively. The inset shows representative staining for each panel. The merged view shows that nuclear fragmentation corresponded to apoptosis (bar, 20 μM). Shown in **a** are the representative results of two independent experiments with pSS patients

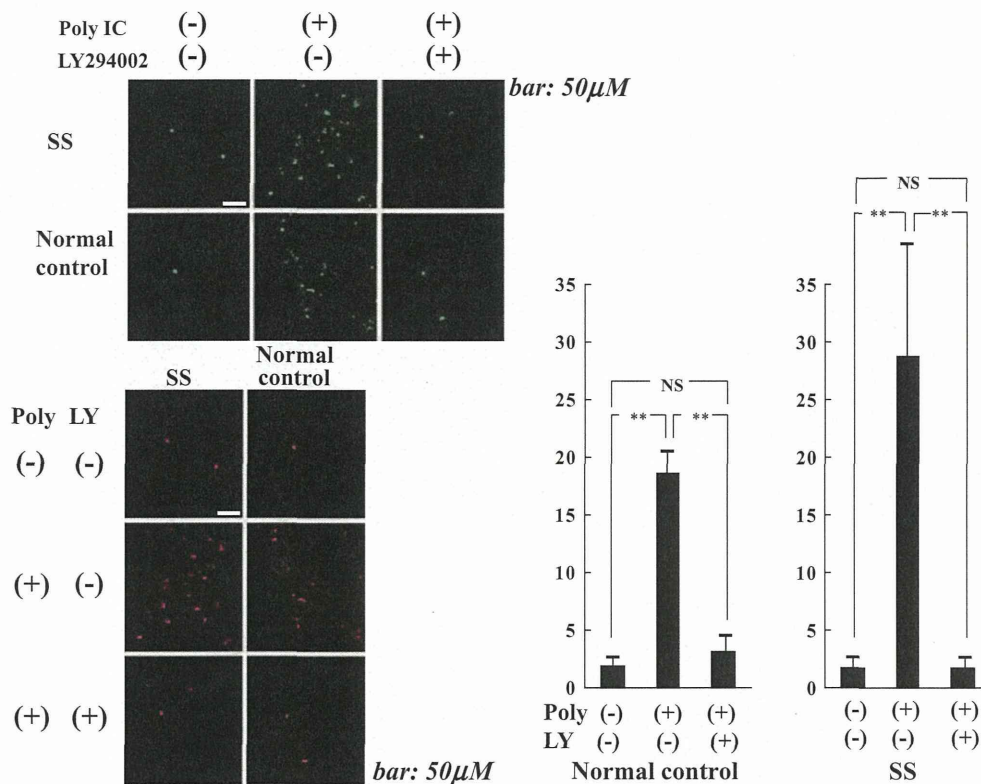


Fig. 4 Quantification of terminal deoxynucleotidyltransferase-mediated dUTP nick end-labeling (TUNEL)-positive apoptotic cells in primary cultured salivary gland epithelial cells (SGECs). After 12 h of starvation of growth supplement, primary cultured SGECs were treated with 25 $\mu\text{g}/\text{ml}$ of poly (I:C) for 24 h. The TUNEL staining image from a pSS patient and a normal subject (*upper panel*) was merged by Hoechst staining (merged view; bar, 50 μM). Then, poly (I:C)-induced apoptosis with or without 50 μM of the PI3K

inhibitor, LY294002, was detected by TUNEL staining (green) in pSS patients and a normal control, followed by quantification with WinROOF software (pink signal) (*lower panel*). The calculated areas of the captured signals were statistically compared using unpaired Student's *t* test ($p < 0.05$; statistically significant) (*right panel*). NS not significant. Shown are the representative results of two independent experiments

staining (Fig. 3a). Furthermore, poly (I:C)-induced TUNEL-positive cells had merged, as determined by Hoechst staining in the SGECs from one normal subject (Fig. 3b). Poly (I:C)-induced apoptosis detected by TUNEL staining (Fig. 4, upper panel) in pSS patients and the normal control was quantified by converting the TUNEL-positive signal (green) into a pink signal, as observed with an image analyzer (Fig. 4, lower panel); significant acceleration of poly (I:C)-induced apoptosis was seen, as was subsequent inhibition by the addition of a PI3K inhibitor, LY294002, in both groups (Fig. 4, right panel). There was also significant difference of poly (I:C)-induced apoptosis between in both groups ($p < 0.01$).

Akt phosphorylation at the poly (I:C)-induced apoptotic site

To determine whether the phosphorylation of Akt is associated with the poly (I:C)-induced cell death of SGECs, immunostaining of phosphorylated Akt and TLR3 was performed at the site of nuclear fragmentation

determined by Hoechst staining. In the SGECs from pSS patients, clear expression of TLR3 and phosphorylated Akt was observed in concert with nuclear fragmentation (Fig. 5, left panel). In the normal subject, poly (I:C)-induced expression of TLR3 and phosphorylated Akt was observed at the site of nuclear fragmentation (Fig. 5, right panel). In the normal subject, poly IC-induced expression of TLR3 and phosphorylated Akt was also observed in cells lacking nuclear fragmentation (Fig. 5, lower panel), which was similar to the co-expression of TLR3 and phosphorylated Akt found in patients with pSS described in Fig. 1b.

Poly (I:C)-induced MAP kinase cleavage of caspase 3 and reversal of effect by PI3K inhibitor

Poly (I:C)-induced expression of MAP kinases including phosphorylated stress-activated protein kinase/Jun-terminal kinase (SAPK/JNK), phosphorylated p38 MAP kinase, and phosphorylated p44/42 MAP kinase was performed. Phosphorylation of SAPK/JNK and p44/42 MAP kinase

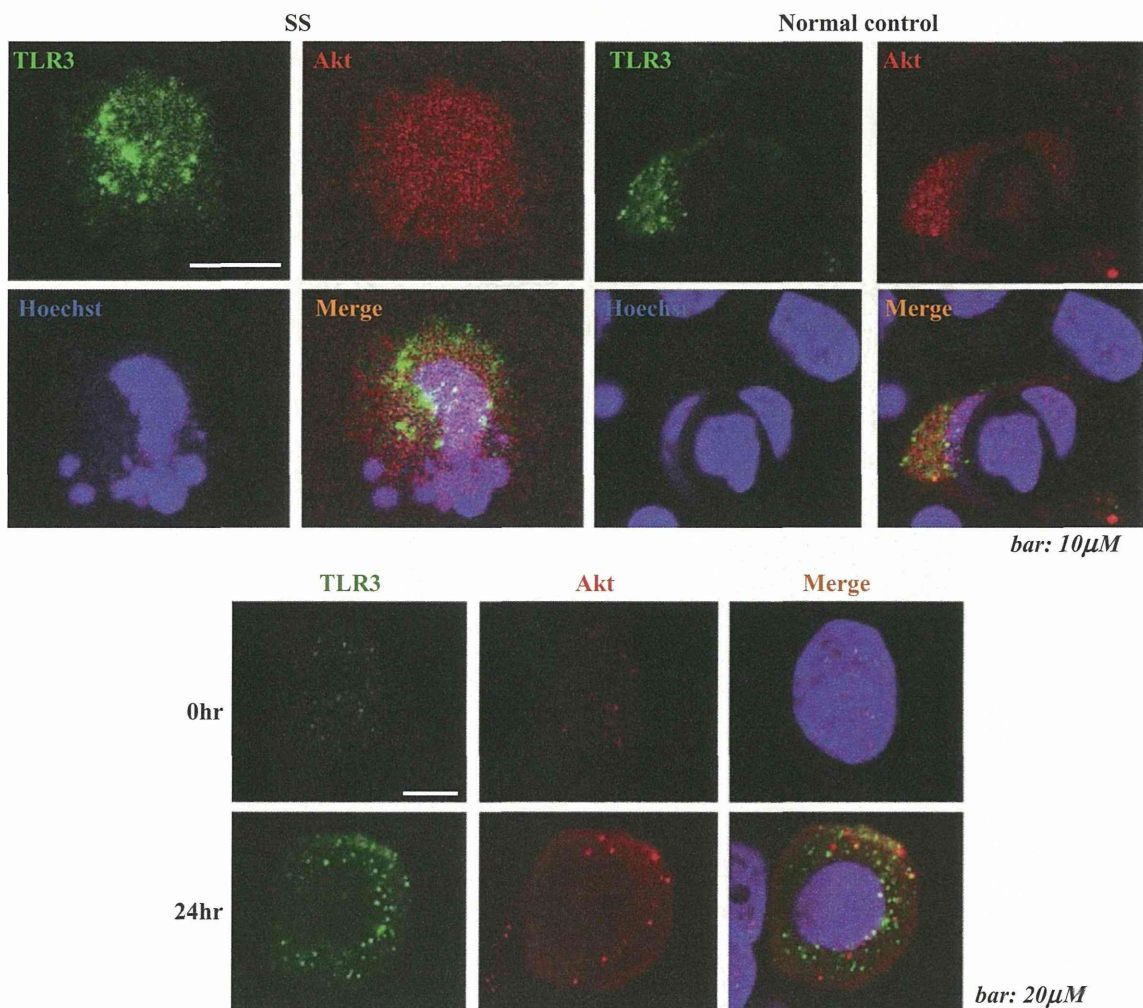


Fig. 5 Co-expression of TLR3 and phosphorylated Akt in apoptotic cells in primary cultured salivary gland epithelial cells (SGECs). After 12 h of starvation of growth supplement, primary cultured SGECs were treated with 25 $\mu\text{g}/\text{ml}$ of poly (I:C) for 24 h with or without 50 μM of the PI3K inhibitor LY294002. Nuclear fragmentation detected by Hoechst staining from a pSS patient (*left panel*) and a normal subject (*right panel*) was observed, and the results of Hoechst staining were merged with double-labeled samples using goat anti-TLR3 antibody with FITC-conjugated secondary antibody

(*green*), and rabbit anti-phosphorylated Akt antibody with tetramethyl rhodamine isothiocyanate (TRITC)-conjugated secondary antibody (*red*). (*Bar* 10 μM). Shown are the representative results of two independent experiments. The *lower panel* shows the expression of TLR3 along with phosphorylated Akt in primary cultured SGECs treated with 25 $\mu\text{g}/\text{ml}$ poly (I:C) for 24 h in a normal subject. (*Bar* 20 μM). Shown are the representative results of two independent experiments with pSS patients

was observed, although phosphorylation of p38 was not found. In addition, poly (I:C)-induced signal of phosphorylated SAPK/JNK and p44/42 MAP kinase in pSS was stronger than that in a normal subject. Slight phosphorylation of Akt induced by poly (I:C) was also found. Poly (I:C)-induced cleavage of caspase 3 was examined by Western blot analysis (Fig. 6). Poly (I:C) stimulation clearly revealed cleavage of caspase 3 in the pSS-SGEC lysate by Western blotting, and this result was also obtained in the case of the lysate from the normal subject. Furthermore, cleavage of caspase 3 induced by poly (I:C) was reversed by the addition of LY294002.

Discussion

In this study, TLR-induced apoptosis was clearly observed in the SGECs of pSS patients, as well as in a normal subject. Hsu et al. [15] initially demonstrated that TLRs had the potential to induce MyD88-independent apoptosis in the presence of the protein kinase PKR. Liew et al. [16] reported that TLR2, TLR3, and TLR4 could induce caspase-dependent or -independent apoptosis, in which MyD88-dependent and TIR domain-containing adaptor-inducing IFN β (TRIF)-dependent pathways were initiated. In addition, Khvalevsky et al. [10] reported that TLR3

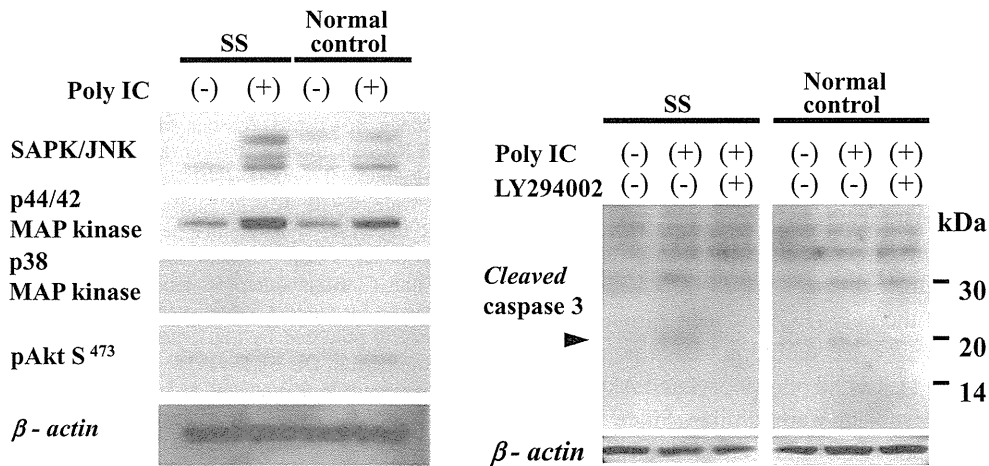


Fig. 6 Detection of poly (I:C)-induced mitogen-activated protein (MAP) kinases and cleavage of caspase 3 in the presence of PI3K inhibitor in primary cultured salivary gland epithelial cells (SGECs). Primary cultured SGECs from a pSS patient or a normal subject were treated with 25 μ g/ml of poly (I:C) for 24 h. Then, poly (I:C)-induced expression of Akt and mitogen-activated protein kinases including phosphorylated-stress-activated protein kinase/Jun-terminal kinase (SAPK/JNK), phosphorylated-p38 MAP kinase, and

phosphorylated-p44/42 MAP kinase was determined by Western blotting (Fig. 6 left panel). With or without 50 μ M of the PI3K inhibitor LY294002, primary cultured SGECs from a pSS patient or a normal subject were treated with 25 μ g/ml of poly (I:C) for 24 h. Then, poly (I:C)-induced cleavage of caspase 3 was determined by Western blotting (Fig. 6 right panel). As a control, β -actin was used. Shown are the representative results of two independent experiments with pSS patients

signaling also induced apoptosis in specific cell lines. Usually, in TLR3 signaling, TRIF is recruited after ligand binding, followed by the activation of NF- κ B [17] and interferon (IFN) regulatory factor 3 (IRF3). However, some cell lines showed no induction of NF- κ B or IRF3; instead, TLR3-dependent cell death was induced in these cell lines. However, in the report [10] by Khvalevsky and co-workers, higher levels of poly (I:C)-induced apoptosis were observed in a colon adenocarcinoma cell line, HepG2, then in a hepatoma cell line, Huh7, or in a human embryonic kidney cell line, HEK293, which suggested that sensitivity to poly (I:C) might be cell-species specific. One explanation for such a difference in apoptotic sensitivity was suggested by Meylan et al. [18], who previously noted that RIP1 activity was required in TLR3 signaling, which indicated that in some cell species, the ability of RIP1 to induce caspase activation was impaired.

With regard to the involvement of Akt in TLR3 signaling, Sarkar et al. [19] revealed that the PI3K-Akt pathway was crucial for TLR3-mediated double-strand RNA-induced genes such as ISG56. Sarkar and colleagues demonstrated that TLR3 downstream of IRF3 was not fully phosphorylated when recruitment of PI3 kinase to TLR3 was blocked, suggesting an essential role for the PI3K-Akt pathway in the TLR3-mediated innate response. Inhibition of PIK3 by a specific inhibitor, LY294002, was followed by clearly impaired TLR3-mediated signaling. In our experiment, phosphorylation of Akt was accompanied by poly (I:C)-induced apoptosis of SGECs. It remains unclear why

the phosphorylation of Akt was correlated with the apoptotic process; however, the downstream signal following the adaptation of TRIF to TLR3 might be involved in the phosphorylation of Akt, coupled with RIP1 activation, which is known to lead to the cleavage of caspase.

Proapoptotic signals in pSS have been reported in previous studies of Fas/Fas ligands, i.e., granzyme/perforin cytotoxic granules generated by CD8+ cytotoxic T lymphocytes [20–24]. As we have reported recently, in cultured SGECs, the Fas/Fas ligand system is well understood [7, 8], and the Fas signal accompanying PI3K inhibition is known to have the potential to induce apoptosis. Furthermore, we recently revealed a rapid induction of apoptosis by tumor necrosis factor (TNF)-related apoptosis-inducing ligand (TRAIL) in the SGECs of pSS [8]. As regards TLR3-mediated cell death in patients with pSS, Manoussakis et al. [25] recently reported that detachment-induced apoptosis was observed in poly (I:C)-treated SGECs from patients with SS. However, the innate immunity-related induction of apoptosis and the anti-apoptotic system in pSS has not yet been fully elucidated. Although no direct association with SS was observed, Numata et al. [26] more recently demonstrated TLR3-mediated apoptosis of human bronchial epithelial cells. Their study clearly showed that insulin-dependent PI3K-Akt signaling inhibited TLR3-mediated cell death. Thus, their results might help elucidate the role of the PI3K-Akt pathway as an anti-apoptotic process in TLR3-mediated cell death. Here, another possibility except TLR3 to induce apoptosis can be considered because TLR3

expression was observed after 24-h stimulation with poly (I:C). Since poly (I:C) also strongly induced melanoma differentiation-associated gene-5 or retinoic acid-induced protein I [27], these mechanisms should be concerned in the apoptotic process of SGEc in SS. The present study suggests a new mechanism to account for salivary gland cell death. The detailed relationship between PI3K-Akt signaling and molecules downstream of the ligation with TLR3 remains supported by the evidence, since PI3K-Akt appears to act as an inducer of the poly (I:C)-induced apoptotic cell death of SGEcs. However, we should note that poly (I:C)-induced expression of TLR3 and phosphorylated Akt in pSS patients and a normal subject were similar. Since the difference was found in poly (I:C)-induced MAP kinases and apoptosis, the phenomenon might explain difference of sensitivity toward pro-apoptotic signal in both groups. Phosphorylation of MAP kinases induced by poly (I:C) is different due to cell species or time course. For example, phosphorylation of p38 is found in corneal fibroblasts at 60-min stimulation with poly (I:C) [28].

In summary, we focused on TLR3-induced apoptosis and the associated phosphorylation of Akt in pSS. These findings may provide novel insights into the apoptotic and anti-apoptotic systems found in the labial salivary glands in pSS. However, the precise signals downstream of TLR-3 have yet to be determined. Downstream signal analysis and related investigations will be necessary to elucidate TLR3-mediated apoptosis of SGEcs in pSS.

Acknowledgments The authors would like to thank Dr. Noriyoshi Ogawa from the Third Department of Internal Medicine at Hamamatsu Medical University for advice regarding the primary cell culture of epithelial cells obtained by minor salivary gland biopsy.

References

- Kawai T, Akira S (2010) The role of pattern-recognition receptors in innate immunity: update on Toll-like receptors. *Nat Immunol* 11:373–384
- Akira S (2006) TLR signaling. *Curr Top Microbiol Immunol* 311:1–16
- Takeuchi O, Akira S (2010) Pattern recognition receptors and inflammation. *Cell* 140:805–820
- Kawakami A, Nakashima K, Tamai M, Nakamura H, Iwanaga N, Fujikawa K et al (2007) Toll-like receptor in salivary glands from patients with Sjögren's syndrome: functional analysis by human salivary gland cell line. *J Rheumatol* 34:1019–1026
- Fox RI (2005) Sjögren's syndrome. *Lancet* 366(9482):321–331
- Nakamura H, Kawakami A, Eguchi K (2006) Mechanisms of autoantibody production and the relationship between autoantibodies and the clinical manifestations in Sjögren's syndrome. *Transl Res* 148:281–288
- Nakamura H, Kawakami A, Ida H, Koji T, Eguchi K (2007) Epidermal growth factor inhibits Fas-mediated apoptosis in salivary epithelial cells of patients with primary Sjögren's syndrome. *Clin Exp Rheumatol* 25:831–837
- Nakamura H, Kawakami A, Iwamoto N, Ida H, Koji T, Eguchi K (2008) Rapid and significant induction of TRAIL-mediated type II cells in apoptosis of primary salivary epithelial cells in primary Sjögren's syndrome. *Apoptosis* 13:1322–1330
- Salaun B, Coste I, Rissoan MC, Lebecque SJ, Renno T (2006) TLR3 can directly trigger apoptosis in human cancer cells. *J Immunol* 176:4894–4901
- Khvalevsky E, Rivkin L, Rachmilewitz J, Galun E, Giladi H (2007) TLR3 signaling in a hepatoma cell line is skewed towards apoptosis. *J Cell Biochem* 100:1301–1312
- Vitali C, Bombardieri S, Jonsson R et al (2002) Classification criteria for Sjögren's syndrome: a revised version of the European criteria proposed by the American-European Consensus Group. *Ann Rheum Dis* 61:554–558
- Nakamura H, Kawakami A, Iwamoto N, Okada A, Yamasaki S, Tamai M et al (2010) A single centre retrospective analysis of AECG classification criteria for primary Sjögren's syndrome based on 112 minor salivary gland biopsies in a Japanese population. *Rheumatology (Oxford)* 49:1290–1293
- Nakamura H, Koji T, Tominaga M et al (1998) Apoptosis in labial salivary glands from Sjögren's syndrome (SS) patients: comparison with human T lymphotropic virus-I (HTLV-I)-seronegative and -seropositive SS patients. *Clin Exp Immunol* 114:106–112
- Nakamura H, Kawakami A, Hayashi T, Iwamoto N, Okada A, Tamai M et al (2010) Anti-centromere antibody-seropositive Sjögren's syndrome differs from conventional subgroup in clinical and pathological study. *BMC Musculoskelet Disord* 11:140
- Hsu LC, Park JM, Zhang K, Luo JL, Maeda S, Kaufman RJ et al (2004) The protein kinase PKR is required for macrophage apoptosis after activation of Toll-like receptor 4. *Nature* 428(6980):341–345
- Liew FY, Xu D, Brint EK, O'Neill LA (2005) Negative regulation of toll-like receptor-mediated immune responses. *Nat Rev Immunol* 5:446–458
- Yamamoto M, Sato S, Hemmi H, Hoshino K, Kaisho T, Sanjo H et al (2003) Role of adaptor TRIF in the MyD88-independent toll-like receptor signaling pathway. *Science* 301(5633):640–643
- Meylan E, Burns K, Hofmann K, Blancheteau V, Martinon F, Kelliher M et al (2004) RIP1 is an essential mediator of Toll-like receptor 3-induced NF-kappa B activation. *Nat Immunol* 5:503–507
- Sarkar SN, Peters KL, Elco CP, Sakamoto S, Pal S, Sen GC (2004) Novel roles of TLR3 tyrosine phosphorylation and PI3 kinase in double-stranded RNA signaling. *Nat Struct Mol Biol* 11:1060–1067
- Kong L, Ogawa N, Nakabayashi T et al (1997) Fas and Fas ligand expression in the salivary glands of patients with primary Sjögren's syndrome. *Arthritis Rheum* 40:87–97
- Matsumura R, Umemiya K, Kagami M et al (1998) Glandular and extraglandular expression of the Fas–Fas ligand and apoptosis in patients with Sjögren's syndrome. *Clin Exp Rheumatol* 16:561–568
- Ohlsson M, Skarstein K, Bolstad AI, Johannessen AC, Jonsson R (2001) Fas-induced apoptosis is a rare event in Sjögren's syndrome. *Lab Invest* 81:95–105
- Tsubota K, Saito I, Miyasaka N (1994) Expression of granzyme A and perforin in lacrimal gland of Sjögren's syndrome. *Adv Exp Med Biol* 1350:637–640
- Kolkowski EC, Reth P, Pelusa F, Bosch J, Pujol-Borrell R, Coll J et al (1999) Th1 predominance and perforin expression in minor salivary glands from patients with primary Sjögren's syndrome. *J Autoimmun* 13:155–162
- Manoussakis MN, Spachidou MP, Maratheftis CI (2010) Salivary epithelial cells from Sjögren's syndrome patients are highly

- sensitive to anoikis induced by TLR-3 ligation. *J Autoimmun* 35:212–218
26. Numata T, Araya J, Fujii S, Hara H, Takasaka N, Kojima J et al (2011) Insulin-dependent phosphatidylinositol 3-kinase/Akt and ERK signaling pathways inhibit TLR3-mediated human bronchial epithelial cell apoptosis. *J Immunol* 187:510–519
27. Gitlin L, Barchet W, Gilfillan S, Cella M, Beutler B, Flavell RA et al (2006) Essential role of mda-5 in type I IFN responses to polyriboinosinic:polyribocytidylic acid and encephalomyocarditis picornavirus. *Proc Natl Acad Sci USA* 103:8459–8464
28. Liu Y, Kimura K, Yanai R, Chikama T, Nishida T (2008) Cytokine, chemokine, and adhesion molecule expression mediated by MAPKs in human corneal fibroblasts exposed to poly(I:C). *Invest Ophthalmol Vis Sci* 49:3336–3344

Serum immune complex containing thrombospondin-1: a novel biomarker for early rheumatoid arthritis

The diagnosis of rheumatoid arthritis (RA) is based on classification criteria set by the 2010 RA classification criteria including serological assessment of rheumatoid factor (RF) and anticitrulline-containing protein/peptide (anti-CCP) antibody.^{1 2} Anti-CCP antibody is specific (94–99%) for RA; however, 25% of patients with established RA and 40% of patients with early RA are negative for this marker.^{3 4} Novel biomarkers, especially for early RA and/or for RA lacking RF and anti-CCP antibody markers (ie, seronegative RA) are therefore urgently required. Circulating immune complexes (CICs) present in the human

body are likely to contain many different antigens that may reflect underlying disease, so antigens incorporated into CICs are promising candidates for diagnostic biomarkers. We developed a novel proteomic strategy (immune complexome analysis) to identify and profile antigens in CICs and used this method to analyse CICs in patients with established RA and controls (healthy donors and patients with osteoarthritis).⁵ CIC-associated thrombospondin-1 (TSP-1) was found in 81% and CIC-associated platelet factor 4 (PF4) in 52% of patients with established RA, but neither protein was found in CICs from any of the controls.⁵ Both proteins are known as endogenous inhibitors of angiogenesis⁶⁻⁸; the formation of CICs may promote angiogenesis. We evaluated the diagnostic potential of CIC-associated TSP-1 and CIC-associated PF4 in patients with early RA divided into seropositive and seronegative groups.

Serum samples were collected from 25 disease-modifying antirheumatic drug (DMARD)-naïve seropositive patients with early RA (mean±SD age 52.8±18.4 years; 21 women; disease duration 0.25–12 months; CRP 0.01–8.55 mg/dl) and 15 seronegative patients with early RA (mean±SD age 60.5±17.9 years; 8 women; disease duration 1–6 months; CRP 0.02–14.4 mg/dl) at Nagasaki University Hospital. All the seropositive patients were positive for RF and 20 were positive for anti-CCP antibody, while all the seronegative patients were negative for both RF and anti-CCP antibody. The diagnosis of RA was made by the 2010 RA classification criteria as well as administration of DMARDs within the first 12 months.^{1, 2} Serum samples from 16 patients with Sjögren's syndrome (SS) (mean±SD age 60.9±13.0 years) and 14 patients with systemic lupus erythematosus (SLE) (mean±SD age 42.6±12.4 years) who fulfilled the international criteria for the diagnosis of SS⁹ and SLE¹⁰ and 11 healthy donors (mean±SD age 49.5±10.3 years) were used as controls. CICs purified by magnetic beads with immobilised protein G were reduced and alkylated, followed by tryptic digestion. The peptide mixture (1 µl) was subjected to nano-liquid chromatography/electrospray ionization/tandem mass spectrometry. More details of the analytical method can be found in our earlier report.⁵

As shown in table 1, CIC-associated TSP-1 was found only in patients with early RA and was not found in disease controls (patients with SS or SLE) or healthy donors (100% specific). Twenty-two (55%) of the total of 40 patients with early RA (56% (14/25) of the seropositive patients and 53% (8/15) of the seronegative patients) had CIC-associated TSP-1. PF4-containing CICs were found in only three patients (8%) with early RA compared with 52% of the patients with

established RA.⁵ These PF4-containing CICs may therefore promote disease progression.

In conclusion, we have shown that CIC-associated TSP-1 has high potential as a novel biomarker for diagnosing early and/or seronegative RA. Further analyses using a large number of patients are warranted to determine the clinical benefit of using this novel biomarker.

Kaname Ohyama,^{1,2} Atsushi Kawakami,³ Mami Tamai,³ Miyako Baba,¹ Naoya Kishikawa,¹ Naotaka Kuroda¹

¹Department of Environmental and Pharmaceutical Sciences, Graduate School of Biomedical Sciences, Nagasaki University, Nagasaki, Japan

²Nagasaki University Research Centre for Genomic Instability and Carcinogenesis (NRGIC), Nagasaki, Japan

³Unit of Translational Medicine, Department of Immunology and Rheumatology, Graduate School of Biomedical Sciences, Nagasaki University, Nagasaki, Japan

Correspondence to Naotaka Kuroda, Department of Environmental and Pharmaceutical Sciences, Graduate School of Biomedical Sciences, Nagasaki University, 1-14 Bunkyo-machi, Nagasaki 852-8521, Japan; n-kuro@nagasaki-u.ac.jp

Funding This work was supported by Special Coordination Funds for Promoting Science and Technology from Japan Science and Technology Agency, a Grant-in-Aid for Young Scientist (B; grant no. 22790160), Challenging Exploratory Research (grant no. 23659301) and Scientific Research (C; grant no. 23591439) from the Ministry of Education, Culture, Sports, Science and Technology of Japan.

Competing interests None.

Ethics approval This study was conducted with the approval of the Institutional Review Board of Nagasaki University.

Provenance and peer review Not commissioned; externally peer reviewed.

Received 4 January 2012

Accepted 19 April 2012

Published Online First 7 June 2012

Ann Rheum Dis 2012;**71**:1916–1917.

doi:10.1136/annrheumdis-2012-201305

REFERENCES

1. **Aletaha D**, Neogi T, Silman AJ, *et al*. 2010 Rheumatoid arthritis classification criteria: an American College of Rheumatology/European League Against Rheumatism collaborative initiative. *Arthritis Rheum* 2010;**62**:2569–81.
2. **Aletaha D**, Neogi T, Silman AJ, *et al*. 2010 rheumatoid arthritis classification criteria: an American College of Rheumatology/European League Against Rheumatism collaborative initiative. *Ann Rheum Dis* 2010;**69**:1580–8.
3. **van Venrooij WJ**, Zendman AJ. Anti-CCP2 antibodies: an overview and perspective of the diagnostic abilities of this serological marker for early rheumatoid arthritis. *Clin Rev Allergy Immunol* 2008;**34**:36–9.
4. **Somers K**, Geusens P, Elewaut D, *et al*. Novel autoantibody markers for early and seronegative rheumatoid arthritis. *J Autoimmun* 2011;**36**:33–46.
5. **Ohyama K**, Ueki Y, Kawakami A, *et al*. Immune complexome analysis of serum and its application in screening for immune complex antigens in rheumatoid arthritis. *Clin Chem* 2011;**57**:905–9.
6. **Jou IM**, Shiau AL, Chen SY, *et al*. Thrombospondin 1 as an effective gene therapeutic strategy in collagen-induced arthritis. *Arthritis Rheum* 2005;**52**:339–44.
7. **Lawler J**. Thrombospondin-1 as an endogenous inhibitor of angiogenesis and tumor growth. *J Cell Mol Med* 2002;**6**:1–12.
8. **Maione TE**, Gray GS, Petro J, *et al*. Inhibition of angiogenesis by recombinant human platelet factor-4 and related peptides. *Science* 1990;**247**:77–9.
9. **Vitali C**, Bombardieri S, Jonsson R, *et al*. Classification criteria for Sjögren's syndrome: a revised version of the European criteria proposed by the American-European Consensus Group. *Ann Rheum Dis* 2002;**61**:554–8.
10. **Cohen AS**, Fries JF, Winchester RJ, *et al*. The 1982 revised criteria for the classification of systemic lupus erythematosus. *Arthritis Rheum* 1982;**25**:1271–7.

Table 1 Number of patients with early RA carrying CIC-associated TSP-1 or CIC-associated PF4

	Early RA patients (n=40)				Healthy donors (n=11)
	Seropositive (n=25)	Seronegative (n=15)	SS patients (n=16)	SLE patients (n=14)	
TSP-1	14	8	0	0	0
PF4	3	0	0	0	0

CIC, circulating immune complex; PF, platelet factor; RA, rheumatoid arthritis; SS, Sjögren's syndrome; SLE, systemic lupus erythematosus; TSP, thrombospondin.

2. 気道感染症

2) HTLV-1 関連気管支病変

屋良さとみ* 山里代利子* 熱海恵理子* 玉寄真紀* 藤田次郎*

Keywords • 成人 T 細胞白血病ウイルス 1 型, 成人 T 細胞白血病, 気管支病変, 呼吸器病変発症病態, 呼吸器病変画像所見/human T-cell leukemia virus type 1 (HTLV-1), human T-cell leukemia (ATL), bronchial disorder, mechanism of respiratory disorder, images of respiratory disorder

要旨 • HTLV-1 は, 成人 T 細胞白血病などの原因ウイルスである。HTLV-1 関連炎症性疾患および HTLV-1 キャリアに HTLV-1 関連肺疾患を認めることが指摘されているが, その病態および発症機序, 臨床所見などについては不明な点が多い。今回 HTLV-1 関連肺疾患の臨床像や画像所見の検討とともに, 発症病態に関与する解析を行った。

1 はじめに

日本はレトロウイルスである成人 T 細胞白血病ウイルス 1 型 (human T-cell leukemia virus type 1: HTLV-1) キャリアの多い国であり, 約 110~120 万人いるといわれ, 約半分が南西九州, 沖縄に存在し, ほかは四国, 紀伊, 北陸, 東北沿岸部にみられる。最近では東京・大阪などの大都市部で症例が増加している。

HTLV-1 ウイルス関連脊髄症やブドウ膜炎症例, 無症候性キャリアで, 肺病変を認めることが以前より指摘されているが, 「HTLV-1 関連肺疾患」とは, 成人 T 細胞白血病 (adult T-cell leukemia: ATL)などを発症していない HTLV-1 キャリアに認められる肺病変を指す場合と, 抗 HTLV-1 抗体陽性者にみられる肺病変すべてを含む概念など確実な定義は確立されていない。キャリアに認められる肺病変に関しては HTLV-1 associated

bronchopneumonopathy (HAB)¹⁾, HTLV-1 associated bronchiolo-alveolar disorder (HABA)²⁾ という名称が提唱されている。その中で病変の画像所見には, 小葉中心性の粒状影を示すびまん性汎細気管支炎 (diffuse panbronchiolitis: DPB) パターン, 慢性気管支炎パターンなどの「気管支病変タイプ」と, usual interstitial pneumonia (UIP) パターンなどの「間質性肺炎 (interstitial pneumonia: IP) タイプ」などのさまざまな報告が散見される³⁾⁴⁾。本稿では文献的考察を交えながら, 主に「HTLV-1 関連気管支病変」を中心に述べていく。

2 HTLV-1 関連気管支病変に関する報告

HTLV-1 関連気管支病変は画像所見が類似の DPB と比較されることが多い。Kadota らはそれらを比較して (HTLV-1 陽性 15 例), 初診時の年齢・性別・臨床症状・一般血液検査・呼吸機能検査・胸部 CT 所見に有意な相違点はなかったと報

HTLV-1 Associated Bronchiolo Disorder

Satomi YARA*, Yoriko YAMAZATO*, Eriko ATSUMI*, Maki TAMAYOSE*, Jiro FUJITA*

* Department of Infections, Respiratory, and Digestive Medicine, Faculty of Medicine, University of the Ryukyus, Okinawa

* 琉球大学大学院医学研究科感染症・呼吸器・消化器内科学講座 (〒903-0215 沖縄県西原町字上原 207)

告した⁵⁾。また気管支肺胞洗浄 (bronchial alveolar lavage : BAL) 液中の IL-2R 陽性細胞が HTLV-1 陽性患者で有意に高値であった。そして DPB に有効なマクロライド少量長期療法は、HTLV-1 関連気管支病変患者においては、15%ほど有用な症例もあるが、その他はほとんど無効であった。

Yamamoto らは HTLV-1 陽性 (12 例) と陰性の DPB 症例を比較し、陽性者で閉塞性換気障害の程度が強く、上葉を侵す割合が高く、また BAL 中の CD3⁺/CD25⁺細胞と CD8⁺/CD25⁺細胞の割合が高く、サイトカイン・ケモカインの MIP-1 α と IP-10 レベルが高かったと報告した⁶⁾。迎らの HTLV-1 陽性 (8 例) と陰性の DPB 症例の比較では、陽性例で BAL 中の CD3⁺/CD25⁺細胞が 2 例で著増、末梢血の CD3⁺/CD25⁺ と CD4/HLA-DR⁺細胞が増加していたが、組織学的な差異は認めなかったとの報告であった⁷⁾。兼島らは HTLV-1 陽性と陰性者との比較で、慢性気道病変として DPB、慢性気管支炎 (chronic bronchitis : CB)、副鼻腔気管支症候群 (sinobronchial syndrome : SBS) などをチェック、HTLV-1 陽性 DPB/陰性 DPB、陽性 CB/陰性 CB との間で比較している。結果として HTLV-1 陽性 CB において、副鼻腔炎の合併率が高い傾向があり、HTLV-1 陽性 DPB/CB において、末梢血のリンパ球幼若化試験で無刺激でも自己増殖を示している症例がみられたが、それ以外の項目においては両者間に大きな違いはなかったと報告している⁸⁾。木村は DPB 様陰影の HABA 症例からはその後 ATL の発症が多く、IP 様陰影の HABA 症例からはその後肺癌の発症が多かったと報告している³⁾。

3 HTLV-1 関連肺疾患の発症機序

HTLV-1 関連肺疾患の病態や発症機序については不明な点が多い。

HTLV-1 の Tax 遺伝子特異的な CD8⁺ T リンパ球による細胞障害性の機序などにより、T リンパ球の肺胞炎やリンパ球性間質性肺炎などの肺病変や各種の臓器障害が起こることがいわれている⁹⁾。また Tax 遺伝子による G1 期での T 細胞の

細胞周期の停止、NF- κ B の活性化による抗アポトーシス作用、p53 の抑制による DNA 損傷修復の阻害や¹⁰⁾、主に CD4⁺ リンパ球に感染した HTLV-1 が肺胞上皮に感染し、NF- κ B、AP-1 を活性化することで発症するという報告もある¹¹⁾。また HTLV-1 に特徴的な pX 領域より生成される TAX 蛋白と HBZ 蛋白は細胞増殖と免疫応答において重要な役割を有している¹²⁾。TAX は NF- κ B、CREB/ATF、AP1 を活性化し T 細胞系増殖を促進することが知られており、これらを介して炎症性サイトカインの発現を促進している。一方 HBZ は無症候性キャリアの T 細胞にも発現し、プロウイルス量と相関が指摘されており、HTLV-1 関連脊髄症の重症度と HBZ の発現は相関も認められている。HBZ は免疫応答からの immune escape にも重要な役割を果たしており、TAX とともに HTLV-1 関連肺疾患の発症と病態に深く関与すると考えられている。

4 当科での HTLV-1 関連肺疾患に関する検討

1) BAL 液解析による検討

HTLV-1 関連 DPB 様症例における BAL 細胞における p40^{tax} (HTLV-1 の非構造蛋白) と各種炎症性サイトカイン、ケモカインの発現とその相関について検討した¹³⁾ (HTLV-1 陽性 DPB 様症例群 10 例 (男性 1 例、女性 9 例; 年齢 60.1 \pm 10.1 歳。図 1 に症例を示す)。コントロール群 7 例 (男性 4 例、女性 3 例; 年齢 53.4 \pm 12.6 歳、抗体陰性、肺陰影なし))。HTLV-1 陽性群ではコントロール群と比べ、BALF 中の総細胞数とリンパ球の割合が有意に増加していた。HTLV-1 陽性群 10 例中 8 例で p40^{tax} の発現が認められ、その発現は BALF 中リンパ球比率と相関している傾向がみられた。またコントロール群に比べ、BALF 細胞中の IFN- γ 、IL-2、MCP-1、MIP-1 α 、IP-10 mRNA の発現が有意に亢進していた。また BALF 細胞中の p40^{tax} の発現が IFN- γ 、MIP-1 α の発現と、IFN- γ と IP-10 の発現がリンパ球比率と有意に相関していた。これらのことから p40^{tax} の発現が局所の炎症性サイトカインやケモカイン産生に関与し、